Determination of the 76 weight % Au section of the Al-Au-Cu phase diagram

F.C. Levey[a,1], M.B. Cortie[b,*,1] and L.A. Cornish[c,2]

[a]*2600 Natta Blvd., Bellmore, NY 11710, USA*
[b]*University of Technology Sydney, PO Box 123, Broadway NSW 2007, Australia*
[c] *Mintek, Private Bag X3015, Randburg 2125, South Africa*

Received ******; accepted ******

Abstract

The substitution of Al for Cu along the 76 wt% Au section of the Al-Au-Cu system causes the α phase of the Au-Cu edge to be successively replaced by a ternary β electron compound, a ternary extension of the Cu-Al γ electron compound, designated here as γ′, and finally the compound $AuAl_2$. A vertical section of this part of the phase diagram has been determined and is presented here, and the relationships between the phases explored. It is considered likely that the section contains the peritectic reactions L+α→β and L+γ′→β. Both the α and the β phases form ordered phases at lower temperatures.

Keywords: A. metals, B. casting, C. X-ray diffraction, E. thermal analysis,

---

1. Introduction

The properties and phase relationships of 18 carat alloys in the Al-Au-Cu system have attracted interest since the early 1990s. This was initially sparked by the development of 'Spangold', a family of jewelry alloys in which a martensitic phase transformation is harnessed to produce an unusual shimmery surface finish [1-3]. The Spangold alloys are designed to contain 76 weight % Au (fractionally more than 18 carats), and variable proportions of Al and Cu. From a metallurgical perspective therefore, a knowledge of the 76% Au vertical section of the ternary Al-Au-Cu system would be useful in terms of understanding the microstructures of these alloys. However, only a scanty prior literature exists on this ternary system, although the binary edges have been well studied, *e.g.* [4-6]. Therefore, we have studied the effect of incremental additions of Al across the 76 wt% Au vertical section, starting at around AuCu and ending at around $AuAl_2$, in order to help explain the structure and properties of the Spangold alloys. Supporting data were obtained from work carried out in parallel on the 500°C isothermal section of Al-Au-Cu [7] and on the trends in color and hardness along the 76% Au section [8]. The results of these studies are used here to construct a proposed vertical section at a constant 76 weight % Au.

Most of the samples studied in this work were annealed for 2 hours only. The vertical section proposed is therefore not a true equilibrium phase diagram, but is nevertheless representative

* Corresponding author. Tel. +61-2-9514-2208; fax: +61-2-9514-7553. *E-mail :* michael.cortie@uts.edu.au
[1] Formerly with Mintek, South Africa
[2] formerly with School of Process and Materials Engineering, University of the Witwatersrand, South Africa

of the phase relationships that would be expected during commercial processing of the alloys. However, a few samples at critical compositions were annealed for appreciable periods of time in an attempt to determine the near-equilibrium phase boundaries as accurately as possible.

For convenience, since the Au content of the alloys remains constant at around 76 wt%, the compositions of the alloys are referred to by their weight % Al contents, with the balance being Cu content.

2. Materials and methods

2.1. Alloy manufacture

Elements of at least 99.9 % purity were used. The samples were weighed out to a precision of ± 0.0005 g and formulated to contain 76 weight % Au. The specimens were made in batches using either arc melting under argon ('first batch') or by melting in a laboratory muffle furnace ('second batch').

The first batch of alloys were weighed out to be either 5g (0 to 7.5% Al at 0.5% Al intervals and an additional 0.25% Al sample) or 10g (7, 8 and 9% Al). Each of the 5g buttons was sectioned into three pieces. One of these was hot-mounted in plastic at 180°C, another was mounted in cold-setting (≤ 80°C) resin, and the third was annealed for five days, quenched into an ice and water mixture, and cold-mounted. The annealing temperature used was 700°C for the 0 to 3.5 % Al buttons and 670°C for the 4.0 to 7.5 % Al buttons. A piece of the nominally 9% Al button was annealed at 500°C for 100 hours in vacuum. Three 0% Al arc-melted buttons were produced. One was annealed at 700°C for 24 hours and quenched in iced water to produce the (Au,Cu) fcc disordered phase. The second button was annealed at 360°C for 24 hours and furnace-cooled to produce the AuCu-I fct ordered phase. The third was left in the as-cast state. All three 0% Al buttons were mounted in hot-setting resin.

The second batch of samples was produced by air-melting. They were weighed out as 10 g each and were made at larger intervals across the entire 76 weight % Au composition range from 0% Al-24% Cu to 24% Al-0% Cu. These alloys were prepared by first melting the Au and then stirring in the other elements. Each alloy was solidified in the crucible, giving a 15 mm diameter disc. A piece of the 2.5 % Al (nominally 3% Al) sample was annealed at 500°C for 100 hours in a vacuum.

A number of samples, taken from both batches, were annealed in muffle furnaces as follows: 400°C for 4 hours, and at 500°C, 600°C and 700°C for 2 hours, followed by an iced brine quench in each case.

2.2. Metallography

The samples were polished to a 0.25 μm finish using a diamond suspension, and some were polished further to a 0.1 μm finish with a gamma alumina suspension. Samples containing 4 to 6 % Al were etched with a chromic acid-based solution[3] prior to metallographic

[3] 0.1g CrO_3 in 10 ml HNO_3 + 100 ml HCl

examination. The other samples were etched in *aqua regia*[4], or were examined in the un-etched condition. Nomarski interference, which shows any surface topography in a highly polished sample, was employed for the examination of the alloys with lower Al contents.

2.3. X-ray diffraction (XRD)

XRD was carried out on the polished surfaces of the samples using Mo k_α radiation. The XRD data collected from the arc-melted buttons had poor count statistics due to the small cross-sectional areas and large grain sizes of the samples. The three pieces of each arc-melted button from the first batch of alloys were therefore arc-melted together to provide a larger sample from which to collect more detailed XRD data. In addition, the 3.0 and 4.5 % Al arc-melted buttons were hot pressed at 750°C to enlarge the available surface area, and then annealed at 700°C for 10 minutes and quenched into iced brine.

The 10 g air-melted discs were examined using custom-made sample holders so that the full surface area of each sample could be exposed to the X-rays. Multiple scans were carried out using different sample orientations and then averaged to minimize the texture effects due to the polycrystalline nature of the samples.

The XRD spectra contained evidence for several known phases (for example AuCu-I, (Au,Cu) and $AuAl_2$) as well as peaks that could not be matched to any phase recorded in the JC-PDS database used (the 1995 edition). The structures of some of the less familiar phases were subsequently determined, and are reported elsewhere [9-11]. The degree of ordering of the AuCu-I phase was primarily determined by computation of the ratio a/c, determined for a four-atom fct ($a/c>1$) or bct unit cell ($a/c<1$).

2.4. Differential thermal analysis (DTA) and composition analysis

Phase transformation temperatures were determined by DTA on a Setaram instrument at a nominal rate of 5K per minute, and by DSC using a Mettler Toledo DSC 821 at 10K per minute.

The compositions of most of the alloys and their constituent phases were determined using EDS in a JEOL 840A 20 kV SEM.

3. Results

3.1. Composition analyses

The overall compositions of the alloys analyzed using EDS are given in Tables 1 and 2. It is evident that roughly 0.3 and 0.4% Al was lost during arc- and air- melting respectively, causing the Au and Cu compositions to be slighter higher than targeted.

[4] 25% by vol. conc. HNO_3 + balance conc. HCl

Table 1: Compositions of 5 and 10g (marked with *) arc-melted samples.

As-weighed wt% Al	Analyzed composition, wt%		
	Au	Cu	Al
0.0	76.3	23.7	0.0
1.0	76.6	22.8	0.6
1.5	76.5	22.2	1.3
2.0	76.9	21.3	1.8
2.5	76.7	21.0	2.3
3.0	76.1	21.0	2.9
3.5	77.1	19.9	3.0
4.0	76.9	19.3	3.8
4.5	77.1	18.5	4.4
6.0	76.6	17.7	5.7
6.5	76.8	17.1	6.1
7.0	76.2	17.0	6.8
7.0*	76.4	17.1	6.5
7.5	76.5	16.3	7.2
8.0*	75.7	16.5	7.8
9.0*	76.3	15.2	8.5

Table 2: Compositions of 10 g air-melted samples.

As-weighed wt% Al	Analyzed composition, wt%		
	Au	Cu	Al
0.0	77.9	22.1	0.0
2.0	77.3	21.2	1.5
3.0	78.3	19.2	2.5
4.0	76.9	19.4	3.7
5.0	77.4	18.2	4.4
7.5	76.8	16.3	6.9
10.0	76.6	13.4	10.0
15.0	78.4	6.5	15.1
20.0	78.0	2.6	19.4
24.0	76.6	0.3	23.1

3.2. The α phase field

Alloys containing 0 % Al were single phase, both after casting, and after annealing at 700°C followed by quenching. X-ray diffraction revealed that these samples were (Au,Cu), a solid solution of Au and Cu, with the disordered $A1$ face-centered cubic structure. If subsequently aged, the samples developed the ordered face-centered tetragonal $L1_0$ structure of AuCu-I. Note however that AuCu exhibits a variable degree of ordering in practice, and that furthermore the samples were slightly off-stoichiometric, at $Au_{50.5}Cu_{49.5}$. As expected from the prior literature, the structure, hardness and degree of ordering of these samples was strongly influenced by prior thermal history. For example, after quenching, the samples were

nearly fully disordered with a hardness of 230 VPN and $a/c \approx 1.0$, but a sample that had been furnace-cooled from 360°C possessed a hardness of over 300 VPN and was nearly completely ordered, with $a/c \approx 1.08$. Unfortunately, the smallish samples contained relatively large grains (about 1 mm, compared to the particle size of 37 to 74 μm (200 to 400 mesh [12]) recommended for powder diffraction measurements). This caused both weak peak intensities in the diffraction spectra and peak heights that differed somewhat from the predicted spectra due to texture effects. Nevertheless, the match between the lattice parameters (determined from peak *positions*) and those listed in the literature (e.g. Pearson's Handbook [6]) for AuCu-I and (Au,Cu) was good. The (Au,Cu) phase field with its ordered derivatives AuCu-I and AuCu-II is referred to here as the 'α phase'.

Aluminum exhibited some solubility in the α phase, with that of as-cast, arc-melted alloys containing up to 1.8 %. In the annealed and quenched arc-melted samples, the Al content of the α increased to 3.8 % Al. The significant difference in Al content of the α phase between these two conditions is indicative of a sloping α phase boundary as observed on the vertical section studied here.

Solid state phase reactions (presumably ordering reactions) between about 340 and 405°C were detected with DTA in the arc-melted 1.8 and 2.3 % Al alloys, suggesting that AuCu was formed in this composition range.

The addition of up to 1% aluminum significantly changed the nature of the hardening in the α phase. For example, while the binary Au-Cu alloy could be readily hardened in the as-cast state, samples with 0.25, 0.50, 1.0 and 1.5% Al were soft in the as-cast and aged state. They apparently required a prior solution anneal at 700°C, followed by a water quench, in order to induce the susceptibility to aging. However, once treated this way, they aged rapidly at temperatures of less than 100°C, producing similar hardnesses to the binary alloy. This unusual effect of Al has been reported previously by Ohta *et al.* [13,14], who describe Al as an age-hardening *accelerator*. On the other hand, according to Raub and Walter [15] the addition of 1.8 wt.% Al had little effect on the (Au,Cu)→AuCu-II→AuCu-I ordering temperatures and on the lattice parameters of those phases. From this it is evident that the effect of Al is not simple, and is evidently related to how much of it is in solution at the time the ageing treatment is initiated.

The modest effect of Al on the lattice parameters of the α phase was confirmed using a custom-written program, described elsewhere [9]. The change in lattice parameter, *a*, of the disordered Au-Cu phase with Al additions is detailed in Table 3. Within experimental scatter, the lattice parameter appears to have inflated only very slightly up to Al contents of 1.8 wt.%, in agreement with the verdict of Raub and Walter [15]. For comparison, the value of *a* listed in the literature for (Au,Cu) with 1:1 stoichiometry varies from 0.387 nm [16] to 0.388 nm [6].

Table 3: Lattice parameters of 5 g arc-melted alloys containing up to 1.8 wt% Al.

Al, wt. %	a, nm	c, nm	(111) d-spacing, nm
0	0.3870±0.0005	0.3820±0.0005	0.2191
nominally 0.25	0.3870±0.0010	= *a*	0.2234
0.6	0.3865±0.0004	= *a*	0.2231
1.3	0.3910±0.0005	0.3810±0.0005	0.2238
1.8	0.3880±0.0004	= *a*	0.2240

The as-cast, arc-melted ternary alloys containing between 1.5 and 3.0 % Al had cored dendritic microstructures (Figure 1 (a)), presumably due to the wide solidification gap (in respect of both temperature and composition) exhibited by these alloys, as shown later in the proposed vertical section. This is likely to have been further exaggerated if the composition of the last liquid to solidify migrated down the liquidus slope of the ternary system to an ultimate position lying away from the 76% Au vertical section. An air-melted 1.5 % Al sample that had been annealed at 500°C for two hours was found to be still cored, although the application of XRD showed that it was comprised substantially or entirely of the α phase. These single phase structures were very resistant to etching.

Some twinning was evident in the 0.6 to 1.8 % Al arc-melted and annealed samples. A greater number of twins appeared with increasing Al content, and these bands of twins appeared to broaden into laths in the 2.9 % Al sample. The markings on the samples of lower Al contents were taken to be twins and not slip lines in line with recommendations by Avner [17]. He stated that slip is visible only on the surface of a specimen and evidence of it will therefore be removed by polishing, whereas twins are visible even after the removal of the surface layer as long as the different orientations they create in the crystal are made visible during the metallographic preparation of the specimen.

3.3. The β phase field

Optical microscopy of the arc-melted alloys in the 4.3 to 5.7 % Al range, and of the air-melted alloys containing 4.4 % Al and nominally 6 % Al, revealed that they were ostensibly single phase. However, in most cases this phase exhibited a lathy microstructure (Figure 2). The appearance and morphology of the laths depended on prior thermal history and applied stress. For example, pronounced laths formed in the material around hardness indentations, and in samples that had been cooled slowly after casting, or which had been hot mounted. In contrast, laths were barely evident or absent in the as-cast, arc-melted and unmounted state. X-ray diffraction studies conducted at ambient and elevated temperatures revealed that the lathy phase at room temperature has the structure of a nominally tetragonal martensite [10], the atomic positions of which are further modulated [11]. The parent phase for this martensite is a little-known ternary β electron phase, with the nominal composition $Au_7Cu_5Al_4$ and an *e*/*a* ratio of 1.48 [9]. The reversible transformation between the two structures has been studied, and is reported elsewhere [18]. It is sufficient to say here that the M_s temperature is in the range 10 to 30°C, while the A_s temperature varies between about 55°C and 77°C (Figure 3). The temperatures at which the M_s and A_s reactions occur in this alloy are dependent upon prior thermal history, and in particular on any ageing that has occurred. Furthermore, the reaction to form austenite is barely detectable in material that has been freshly quenched from

700°C.

Studies of the transformation behavior of alloys with between 5 and 6% Al have shown that the most prominent development of laths requires the prior occurrence of $B2 \rightarrow L2_1$-type ordering of the parent phase. This evidently takes place at temperatures between 100 and at least 200°C [9,10,18]. However, it is evidently not the ordering itself that produces the laths but rather a subsequent reversible transformation of the $L2_1$ phase to a lower temperature martensitic derivative. The *B*2 ordering of the parent phase which hosts these phenomena is intact to at least 640°C, at which temperature a reaction occurs (Figure 4), believed to be incipient melting at the grain boundaries. The stability of *B2* ordering up to the melting point in noble metal β-phases is not uncommon [19]. Not even rapid solidification (splat casting onto a copper plate) was able to completely suppress the *B*2 ordering of the present alloys, indicating that it occurs very readily. This ternary phase field, consisting of the high temperature *B*2 crystal structure and its lower temperature $L2_1$ descendent, is referred to as the β phase field here, while the martensite produced by cooling the $L2_1$ phase will be designated as β′. XRD analysis revealed that a mixture of the *B*2 and β´ phases was obtained in as-cast, arc-melted samples, whereas only the β´ phase was produced in as-cast, air-melted or slow cooled samples in this ternary β phase region [18]. Lath formation was suppressed or absent in samples where $L2_1$-ordering had not been allowed to take place (such as in as-cast and un-mounted arc-melted samples, or air-melted samples that had been annealed and quenched), a phenomenon well-known in diverse other noble metal beta phase systems. It should be noted that all of the 5 g arc-melted alloys received a low temperature heat treatment during the (hot or 'cold') mounting process, thereby explaining the presence of β′ in samples that had been ostensibly quenched from elevated temperatures. Evidently these samples had undergone sufficient $L2_1$ ordering during mounting to enable their subsequent transformation to laths of β′.

The β´ phase was very slow to etch in the CrO_3 solution, which however was the only etchant found to produce acceptable micrographs.

3.4. The α + β phase field

At compositions in between the α and β phase fields, the microstructure consisted of dendrites of α in a matrix of β (Figure 1b). These dual phase structures etched readily in the CrO_3 solution, with the β phase becoming deeply etched within a relatively short period of time. With appropriate heat treatment, β′ laths formed in the β matrix. The presence of two phases, α and β′, was confirmed with XRD.

The composition range of this two-phase region was affected by the prior thermal history of the samples due to a strong temperature dependence of the constituent phase stability at elevated temperatures, as illustrated later in the proposed vertical section. The α / α+β and α+β / β phase boundaries were plotted from results of EDS phase analyses of various samples annealed at elevated temperatures. It is evident that these phase boundaries slope steeply at high temperatures, so both the cooling rate during solidification and after annealing will affect the observed microstructure.

Furthermore, it was evident that a phase transformation was taking place. Annealing of the dual-phase samples at temperatures from 400 to 600°C caused the alpha dendrites to shrink at

the expense of an enlarging proportion of the β matrix (Figure 5). This suggests that under equilibrium conditions, the β is formed peritectically from α + liquid. In addition, Widmanstätten-like needles of β phase precipitated within the residual α, once again implying a sloping α / β phase boundary.

3.5. Alloys containing between 6 and 8 % Al

A fine duplex structure was apparent in the 6.1 to 7.5 % Al arc-melted samples in both the as-cast state and after annealing at 670°C (Figure 1c). Occasional patches of laths were also present in the 6.1 and the 6.8 % Al as-cast arc-melted alloys. The 6.9 % Al air-melted sample contained a minor pinkish interdendritic component. EDS analysis of the coarser regions of the duplex structure indicated that there was a consistent compositional variation between the dendritic and interdendritic regions of these samples, as indicated in Table 4.

Table 4: EDS phase analyses of 6.9 and 7.2 % Al samples annealed at 500°C.

Overall wt% Al	Phase analysed	Weight %			Atomic %		
		Au	Cu	Al	Au	Cu	Al
6.9	dendrite	75.8	16.5	7.7	41.4	28.0	30.6
	matrix	79.2	15.0	5.8	47.1	27.6	25.3
7.2	dendrite	75.4	16.9	7.7	41.0	28.4	30.6
	matrix	78.6	15.3	6.1	46.1	27.9	26.0

Since the two-phase structure in the 6.1 to 7.5 % Al samples did not disappear with extended annealing periods, it would appear that it is a near-equilibrium structure. This would exclude the possibility of coring due to rapid cooling from a solid + liquid phase region. Close examination revealed that the proportion of the dendritic phase grew with increasing Al content between 6 and 7.5 % Al, and that the 7.8% Al sample appeared to be completely comprised of it. The 7.8 % Al arc-melted sample was single phase in both the as-cast condition and after annealing for 4 hours at 500°C. The XRD spectra of this sample revealed that the structure of the phase was similar to that of the Al_4Cu_9 γ phase, although with a degree of ternary ordering [7]. The stoichiometry can be expressed as $Al_4(Cu_{0.4}Au_{0.6})_9$ and it will be designated here as γ′ to distinguish it from the binary compound. The interdendritic phase was obviously β′, with its characteristic laths and, at its terminal composition, its pinkish hue.

A duplex structure having a morphology of a single interdendritic phase is consistent with that of a peritectic reaction [20] rather than that of a eutectic. Having dendrites of the γ′ phase in a β matrix would indicate the reaction $L + \gamma' \rightarrow \beta$, and this is shown in the proposed vertical section.

3.6. Alloys containing more than 8 % Al

All of the alloys containing more than 8 % Al consisted of two phases – the purple stoichiometric intermetallic phase, $AuAl_2$, and one other. The presence of the $AuAl_2$ phase was exceedingly obvious in the 23.1 % Al alloy which was characterized by the distinctive purple hue of this intermetallic compound. In all of these alloys, the $AuAl_2$ structure contained a little Cu in solution. The small amount of Cu present in the 23.1 % Al sample was presumably picked up from the copper hearth during the arc-melting process since none was added to the original sample.

The alloys containing between 8 and 20 % Al consisted of $AuAl_2$ and γ′ (Figure 1d, e and f). This was confirmed both by XRD of the 10.0 % Al as-cast sample (Figure 6) and by EDS phase analyses of the 8.5, 10.0 and 19.4 % Al samples (Table 5). The 23.1 % Al sample consisted almost entirely of dendrites of $AuAl_2$. There was also a small amount of (Al) present at the grain boundaries. This was confirmed with XRD.

Table 5: EDS phase analyses of samples containing more than 8 % Al annealed at 500°C.

Overall	Phase	Weight %		
Wt% Al	analysed	Au	Cu	Al
8.5	γ′	76.8	15.3	7.9
	$AuAl_2$	78.7	2.5	18.8
10.0	γ′	76.9	14.9	8.2
	$AuAl_2$	78.3	0.3	21.4
19.4	γ′	79.3	12.9	7.8
	$AuAl_2$	78.2	0.9	20.9
23.1	$AuAl_2$	78.3	0.3	21.4
	(Al)	1.9	0.2	97.9

The 8.5% Al arc-melted sample and the 10.0% Al air-melted sample consisted of dendrites of the γ′ phase together with a minor interdendritic component of the $AuAl_2$ phase. The microstructure of these samples had a morphology consistent with that formed by a ‘divorced eutectic’ reaction, which occurs when there is some nucleation difficulty which causes the remaining liquid to solidify separately [20]. In this case, it appears that the γ′ phase was solidified separately on the existing γ′ dendrites and the $AuAl_2$ phase was precipitated interdendritically as a continuous single phase. The section through this proposed eutectic valley was estimated to occur at a slightly higher Al content than that of the 10.0 % Al air-melted alloy, in keeping with the positions of the points on the liquidus line which were determined by DTA.

The 15.1 % and 19.4 % Al samples contained purple $AuAl_2$ dendrites in a divorced $AuAl_2$ + γ′ eutectic structure. The relative proportion of $AuAl_2$ dendrites increased with Al content.

Since the 8.5 % to 19.4 % Al samples consisted only of γ′ and $AuAl_2$ and the 23.1 % Al sample consisted only of $AuAl_2$ and (Al), there must be a region along the vertical section where either only the $AuAl_2$ phase exists, or in which there is a three phase field of $AuAl_2$, γ′ and (Al), which would be the product of a ternary invariant reaction. In fact, the ability of the $AuAl_2$ phase to take up to 2.5 wt% Cu (3.4 atomic % Cu) into its lattice ensures that the former applies. Therefore, as one moves further away from the Al-Au edge along the vertical

section (i.e. with the addition of more Cu), there is a single phase region of the ternary extension of $AuAl_2$, and on the other side of this single phase region, the $\gamma' + AuAl_2$ region begins.

3.7. Construction of the 76 weight % Au vertical section

The DTA data obtained for all of the alloys were interpreted using standard methods [21-23] The liquidus/solidus temperatures were virtually the same for the heating and cooling cycles, indicating that there was minimal superheating or undercooling during these respective cycles [21].

The melting and solidification temperatures determined from the data are shown on a proposed constant 76 weight % Au vertical section of the ternary system in Figure 7. The expected liquidus of the binary 76 wt% Au - 24 wt% Al alloy has been plotted according to the documented binary phase diagram [5], as the alloy melts above the maximum temperature of 950°C used in the DTA. The lower limit of temperature on the diagram is 400°C. This study did not attempt to examine the details of the various ordered forms of AuCu.

It is important to note that although the onset of solidification, *i.e.* the liquidus temperature, will be correct for the vertical section, the solidus temperature read off a cooling curve could be lower than the solidus temperature of the vertical section. This is because the composition of the liquid remaining during the solidification process runs down the steepest slope of the ternary surface, and the path it follows does not necessarily lie in the same vertical plane as the vertical section. The DTA data were thus not interpreted in this vertical section as giving definitive solidus temperatures, but were used together with the information gleaned from the other experiments performed on the alloys in the construction of the proposed vertical section. In addition, the ternary composition surfaces for the liquid and solid phases remaining during the solidification process may well run in different directions in the ternary system. This appears to be the case for the peritectic reaction $L + \gamma' \rightarrow \beta$, as the liquidus in the plane of the vertical section does not slope down towards the peritectic. The fact that both three phase regions, $L + \alpha + \beta$ and $L + \beta + \gamma'$, have the product and (solid) parent phase at different temperatures is an indication that the tie lines do not lie in the vertical section. For the $L + \beta + \gamma'$ phase field, the tie lines must lie at quite a different angle from the vertical section because of the shape of it, whereas for the $L + \alpha + \beta$ field, the shape indicates that the tie lines lie fairly close to the plane of the vertical section.

It should also be remembered that the alloys did not contain exactly 76 weight % Au, due to compositional changes during melting. It follows therefore that the reaction temperatures indicated on the vertical section do not lie exactly in the vertical plane, as would be implied.

EDS phase analyses of various annealed samples were used to construct phase boundaries at temperatures between 400 and 700°C. In general, the tie-lines of these phase analyses do not lie in the plane of the vertical section given in Figure 7. Furthermore, the samples annealed at 400°C were obviously not held at temperature for long enough for the phase reactions to reach completion. The phase boundaries given in the vertical section were therefore drawn as smooth lines, rather than drawn to pass exactly through the Al contents determined by the phase analyses. In addition, the shapes of the phase fields in Figure 7 were drawn as a best-fit of the reaction temperatures determined by DTA, while obeying the thermodynamic laws [23]

and taking the microstructures and phase analyses of the alloys into consideration.

In the region close to the Au-Al edge of the vertical section, there is a two-phase $AuAl_2$ + liquid (L) region at elevated temperatures and a two-phase $AuAl_2$ + (Al) region at lower temperatures, in accordance with the binary Au-Al system. There would also, then, be a three phase region containing L + (Al) + $AuAl_2$, with one apex at the binary eutectic reaction. Moving along the vertical section, away from the Au-Al edge (i.e. with increasing Cu content), the L + $AuAl_2$ region probably extends from this region, above the melting locus of the $AuAl_2$ single phase region, and is contiguous with the L + $AuAl_2$ region on the other side of the $AuAl_2$ single phase region. This is shown by the solid phase boundary of the $AuAl_2$ phase on the proposed vertical section. There is a smaller probability of the $AuAl_2$ phase melting congruently, as shown by the dotted phase boundary. However, the former explanation is more likely because the composition is a little removed from the binary Au-Al composition and the extra degree of freedom of the ternary system would allow non-congruent melting.

The Al-rich phase boundary of the Spangold β phase was taken as close to 6 % Al since a two-phase β′ + γ′ structure was formed at higher Al contents and commercially manufactured slabs containing 6.0 % Al consisted substantially of the Spangold β′ phase. As mentioned, a small endothermic peak was consistently observed at around 640°C in various samples containing nominally 6 % Al, and apparently indicated incipient melting. Molten grain boundaries were also observed while soaking commercially manufactured 6.0 % Al slabs at temperatures between 650 and 700°C. Furthermore, both the nominally 5.5 % (assumed to be about 5.2%) and the 5.7 % Al arc-melted samples melted during the annealing treatments at 670°C. The Al-rich apex of the L + β phase field, on the solidus line, has thus been taken to occur near 635°C and 6.0 % Al.

A single phase region of γ′ has been included at around 7.8 wt% Al, consistent with the single phase microstructure of this sample, with two-phase regions of β + γ′ and $AuAl_2$ + γ′ on either side.

4. Discussion

The 76 weight % Au vertical section of the Au-Cu-Al ternary system is significantly more complex than was originally anticipated when the Spangold alloys were developed. One of the first theories was that the Spangold alloys lay in a ternary extension of the binary AuCu II phase, which exhibits a similar surface morphology [16,24,25]. However, once the structure of the Spangold alloys was shown to be consistent with that of a β electron compound [9,26], it was thought that this could be an extension of either the Au_4Al β phase, or the Cu-Al β phase, which occurs at 70-80 atomic % Cu. It was envisaged that the β phase could even stretch across the ternary system from Au_4Al to the Cu-Al β phase, as in the Au-Ag-Al system [27].

However, it has been shown [7] that, similar to systems such as Al-Au-Ti, Au-Cu-Ti and Au-Cu-Ga [27], amongst others, a region of ternary β phase exists in the Au-Cu-Al system. The Spangold alloys are formulated to fall in this ternary β phase field, the boundaries of which at 500°C and 76 wt% Au, are 2.4 and 6% Al.

Due to the similarity of the X-ray diffraction spectra of the 7.8 % Al and 6% Al alloys (the atomic positions of the γ brass structure are also very roughly in a bcc relationship), and the restricted extent of the duplex γ plus β phase field (it exists only between 6 and 7.8 wt.% Al), it was initially thought that the β phase field extended as far as 7.8 % Al [9,18,26]. However, the Al_4Cu_9 γ phase was subsequently shown to exhibit a surprising amount of Au solubility [7], so that this ternary extension of this phase is intersected at around 7.8 % Al along the vertical section.

There were also some surprises with the nature of the solidification reactions, with a divorced eutectic occurring from around 8 to a little more than 10 % Al, and the slope of the peritectic reaction surface running out of the plane of the vertical section. The tie lines here must be at a large deviation from the plane of the vertical section.

Notwithstanding the above limitations, the experimental observations of the alloys can now be satisfactorily explained using the proposed vertical section. The phase boundaries of the vertical section determined by EDS analysis confirm the optical microscopy observations of as-cast and annealed samples, as well as the hardness and color variations observed for the range of 18 carat alloys [8]. It is hoped that this new understanding will abet further technological advances in the use of these alloys.

5. Conclusions

The Al-Au-Cu ternary system has not been well documented in the literature, and we propose here a first vertical section along the technologically relevant 76 wt% Au line. Starting at the high Cu end, the 76 wt% Au section of the Al-Au-Cu system shows the classic progression of α, β and γ electron phases, before ending with the intermetallic compound $AuAl_2$ at the high Al end.

The α phase exists as a disordered solid solution of Au and Cu at elevated temperatures, but orders to AuCu-I and AuCu-II at lower temperatures. The solubility of Al in the α phase decreases with decreasing temperature. The α phase appears to undergo a peritectic reaction to form β phase between nominal sample compositions of 2%Al and 4%Al.

The β phase has the *B*2 structure at elevated temperatures, possibly up to its melting point, but develops ternary ordering of the $L2_1$ type at temperatures below about 250°C.

The $Al_4(Cu_{0.4}Au_{0.6})_9$ γ′ intermetallic phase on this section is contiguous with the Al_4Cu_9 γ phase of the Cu-Al system. The microstructure of alloys in the narrow β + γ′ phase field suggests the peritectic reaction L + γ′ → β.

A ternary extension of the intermetallic $AuAl_2$ phase is formed at Al contents of 21.5 % to close to 24 % Al along the vertical section. A two-phase region exists between the ternary γ′ phase field and the ternary extension of the $AuAl_2$ phase. The liquidus surface of this two-phase region appears to contain a eutectic valley, which is intersected by the 76 weight % Au vertical section. However, the morphology of the eutectic mixture indicates that it is formed as a "divorced eutectic" in the samples studied.

It is likely that the L + $AuAl_2$ region extends above the ternary extension of the $AuAl_2$ phase,

instead of the $AuAl_2$-based phase melting congruently, as its composition is a little removed from the binary $AuAl_2$ composition. A two-phase $AuAl_2$ + (Al) region exists below a three-phase L + $AuAl_2$ + (Al) phase field at compositions on the vertical section between the ternary $AuAl_2$-based phase and the Au-Al binary.

Acknowledgements
This paper is published by permission of Mintek. The authors wish to thank Mettler Toledo of Switzerland for kindly providing some of the DSC scans used.

6. References

[1] I.M. Wolff, M.B. Cortie, Gold Bulletin, 27 (2) (1994) 44.

[2] I.M. Wolff, V.R. Pretorius, Gold Technology, 12 (1994) 7.

[3] M. Cortie, I. Wolff, F. Levey, S. Taylor, R. Watt, R. Pretorius, T. Biggs, J. Hurly, Gold Technology, 14 (1994) 30.

[4] R. Hultgren, R.L. Orr, P.D. Anderson, K.K. Kelly, Selected Values of Thermodynamic Properties of Metals and Alloys, John Wiley and Sons, New York, USA 1963.

[5] J.L. Murray, H. Okamoto, T.B. Massalski (Eds.), Binary Alloy Phase Diagrams, vol. 1, ASM, Metals Park, Ohio, USA 1987.

[6] P. Villars, L.D. Calvert (Eds.), Pearson's Handbook of Crystallographic Data for Intermetallic Phases, vol. 2, ASM, Metals Park, Ohio, USA 1985, pp. 894, 1190, 1922.

[7] F.C. Levey, M.B. Cortie, L.A. Cornish, Metallurgical and Materials Transactions A, 33 (4) (2002) 987.

[8] F.C. Levey, M.B. Cortie, L.A. Cornish, Scripta Materialia, 47 (2002) 95.

[9] M.B. Cortie, F.C. Levey, Intermetallics, 8 (2000) 793.

[10] F.C. Levey, M.B. Cortie, Materials Science and Engineering A, A303 (2001) 1.

[11] M.B. Cortie, F.C. Levey, Intermetallics, 10 (2002) 23.

[12] L.V. Azároff, Elements of X-Ray Crystallography, McGraw-Hill, New York 1968.

[13] M. Ohta, T. Shiraishi, M. Nakagawa, S. Matsuya, J. Mater. Sci, 29 (8) (1994) 2083.

[14] M. Ohta, S. Matsuya, T. Shiraishi, M. Nakagawa, US Patent 5338378 (1994).

[15] E. Raub, P. Walter, Z. Metall., 41 (1950) 240.

[16] B.C. Muddle, J.F. Nie, G.R. Hugo, Metall. Trans., 25 (1994) 1841.

[17] S.H. Avner, Introduction to Physical Metallurgy, 2nd ed., McGraw-Hill, Singapore 1974, pp.118, 195-202.

[18] F.C. Levey, M.B. Cortie, L.A. Cornish, Metall. and Mater. Trans. A, 31 (2000) 1917.

[19] R.W. Cahn, in Diffusion in Ordered Alloys, Fultz, B. *et al* (ed.), The Minerals, Metals & Materials Society, Warrendale, PA, USA (1993) 125.

[20] G.A. Chadwick, Metallography of Phase Transformations, Butterworths, London 1972.

[21] W. Gutt, A.J. Majumdar, in Differential Thermal Analysis, vol. 2, Mackenzie R.C. (ed.), Academic Press, London, Great Britain 1972.

[22] D.S. Evans, A. Prince, Journal of the Less-Common Metals, 114 (1985) 225.

[23] D.R.F. West, Ternary Equilibrium Diagrams, 2nd ed., Chapman and Hall, London, Great Britain 1982.

[24] R. Smith, J.S. Bowles, Acta Metallurgica, 8 (1960) 405.

[25] J.S. Bowles, C.M. Wayman, Acta Metallurgica, 27 (1979) 833.

[26] F.C. Levey, M.B. Cortie, T. Biggs, P. Ellis, Proceedings of the Microscopy Society of Southern Africa, 28 (1998) 18.

[27] A. Prince, G.V. Raynor, D.S. Evans (Eds.), Phase Diagrams of Ternary Gold Alloys, The Institute of Metals, London, 1990, p.221.

FIGURES

Figure 1. Microstructures of selected as-cast samples on the 76 wt.% Au section of the Al-Au-Cu ternary. a. 2% Al, b. 4% Al, c. 7.5% Al, d. 10% Al, e. 15% Al, f. 20% Al.

Figure 2. Lathy structure of low-temperature form of the β phase.

Figure 3. Low temperature DSC scan of well-aged 5.5% Al alloy, showing reversible martensite (M) and austenite (A) reactions.

Figure 4. DSC scan showing a reversible reaction at about 640°C, presumed to be incipient melting.

Figure 5: Remnants of α dendrites which were eroded by a growing β interdendritic phase while annealing the 3.7 % Al air-melted sample for 4 hours at 400°C.

Figure 6: XRD spectrum of 10.0% Al as-cast sample together with the peak positions of the γ and $AuAl_2$ phases.

Figure 7. Vertical section of the Al-Au-Cu phase diagram at 76 weight % Au. Note that the slope of the liquidus appears to run in the wrong direction for the $L + \gamma \rightarrow \beta$ peritectic reaction as it lies out of the plane of the vertical section.

FIGURES

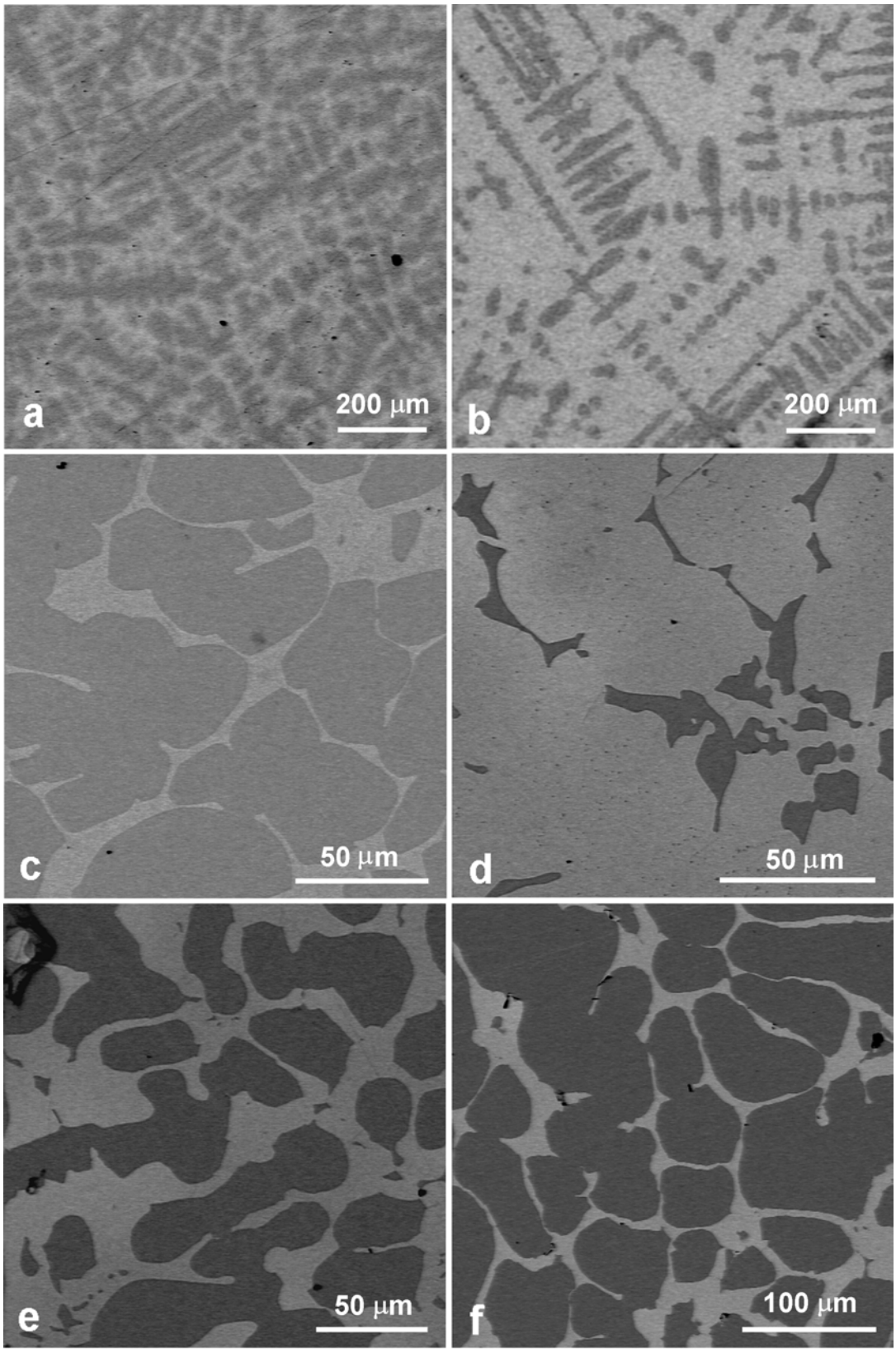

Figure 1. Microstructures of selected as-cast samples on the 76 wt.% Au section of the Al-Au-Cu ternary. a 2% Al, b. 4% Al, c. 7.5% Al, d. 10% Al, e. 15% Al, f. 20% Al

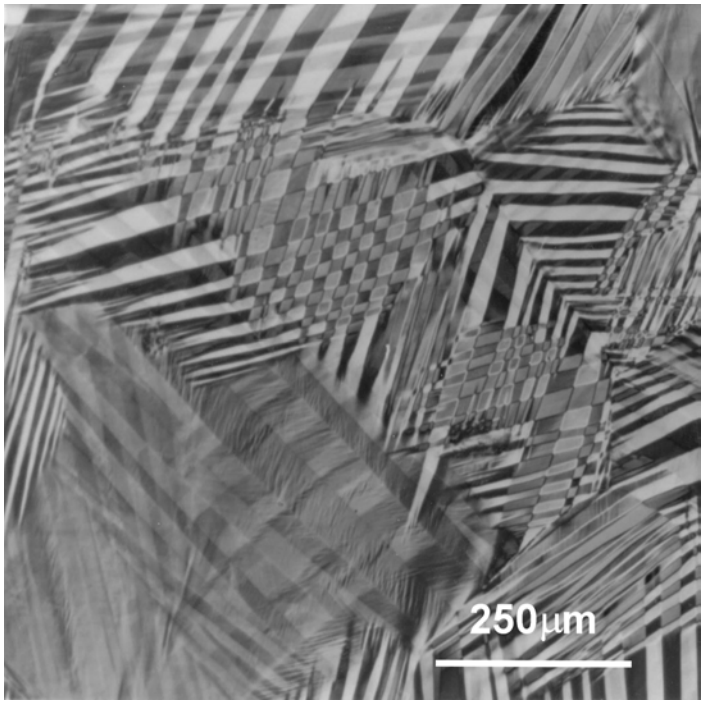

Figure 2. Lathy structure of low-temperature form of the β phase.

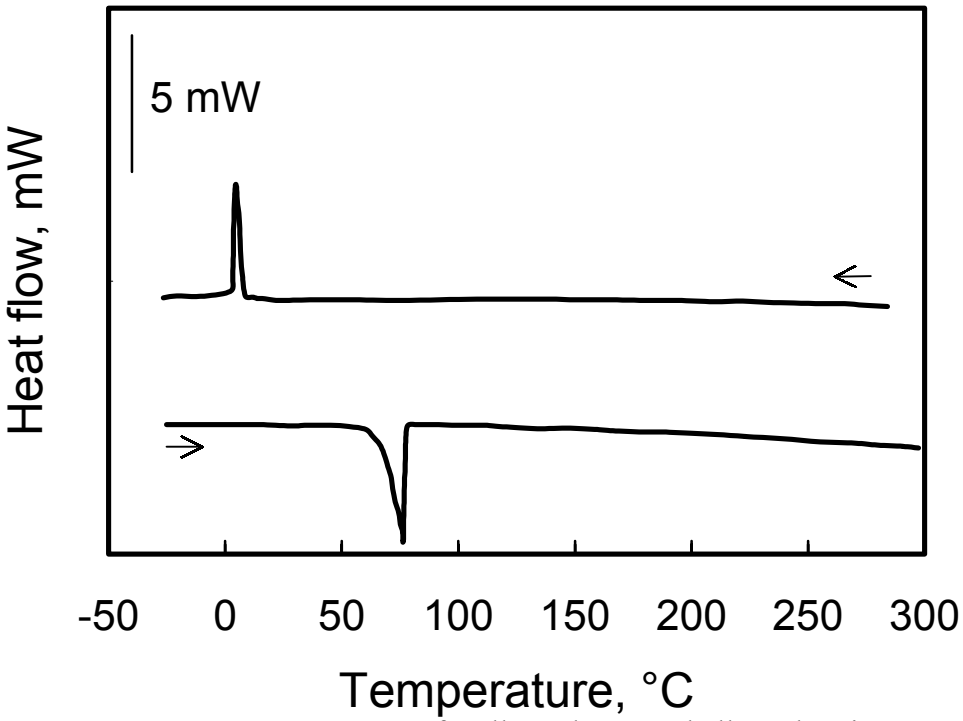

Figure 3. Low temperature DSC scan of well-aged 5.5% Al alloy, showing reversible martensite (M) and austenite (A) reactions.

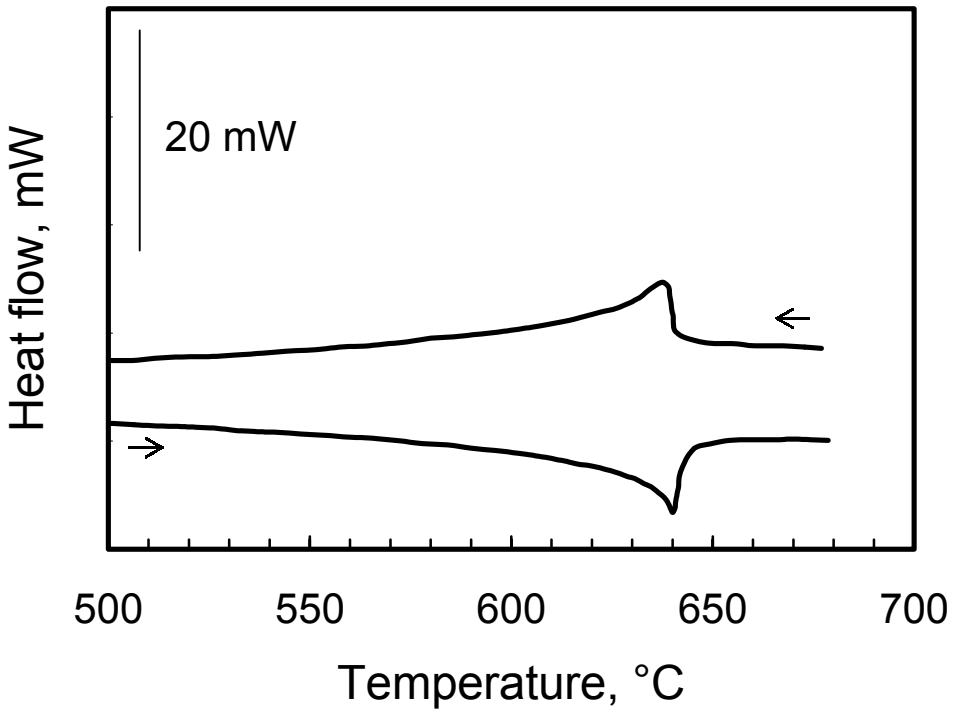

Figure 4. DSC scan showing a reversible reaction at about 630°C, presumed to be incipient melting.

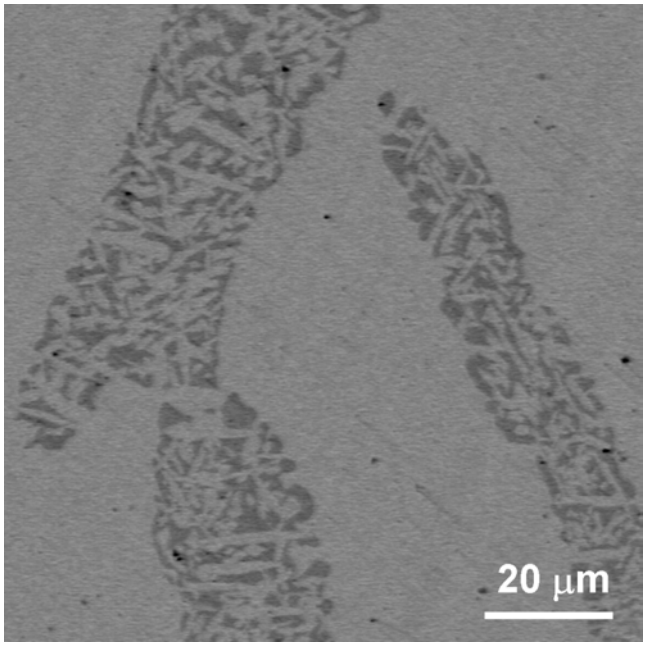

Figure 5: Remnants of α dendrites which were eroded by a growing β interdendritic phase while annealing the 3.7 % Al air-melted sample for 4 hours at 400°C.

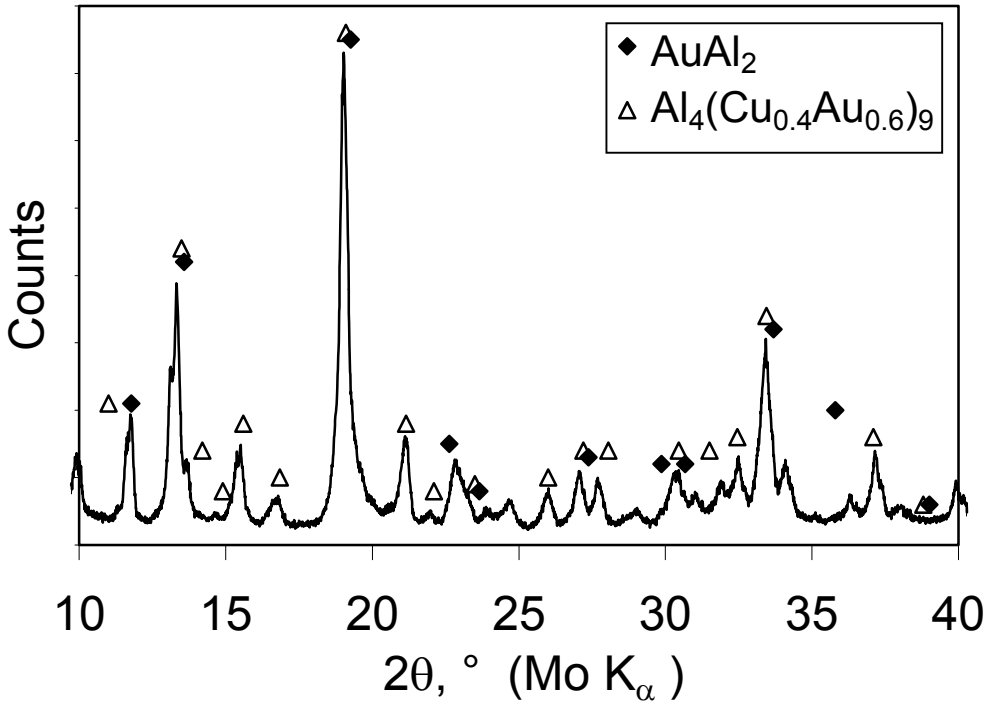

Figure 6: XRD spectrum of 10.0% Al as-cast sample together with the peak positions of the γ and $AuAl_2$ phases.

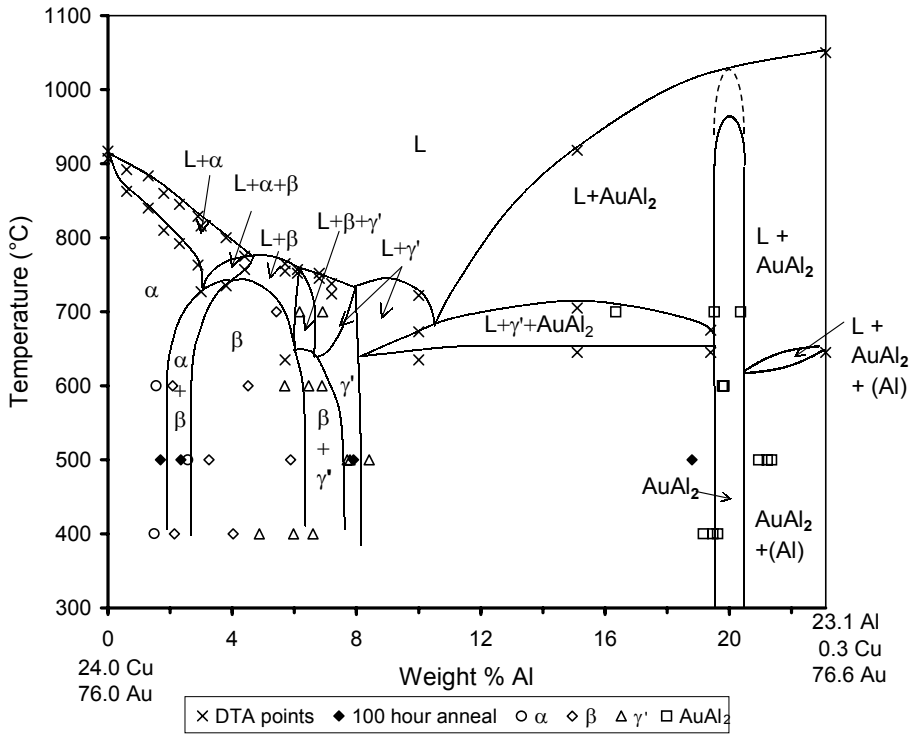

Figure 7. Vertical section of the Al-Au-Cu phase diagram at 76 weight % Au. Note that the slope of the liquidus appears to run in the wrong direction for the L + γ →β peritectic reaction as it lies out of the plane of the vertical section.